## 29.0 IDENTIFICATION OF DEFORMATION MECHANISMS OF THERMALLY STABLE CAST AL-CU ALLOYS *VIA* NEUTRON DIFFRACTION (LEVERGARED)

Brian Milligan (CSM)
Faculty: Amy Clarke (CSM)
Industrial Mentor: Amit Shyam (ORNL)

### 29.1 Project Overview and Industrial Relevance

Cast Al-Cu alloys have great industrial importance due to their low cost, high strength, and ease of manufacturing. However, they still run into several problems. One such problem relevant to many applications of Al-Cu alloys is the loss of strength during high temperature exposure, such as in advanced internal combustion engines. This phenomena has been studied extensively in the past using microscopy [29.1] and mechanical testing [29.2]. While most previous studies have focused on bulk mechanical properties, the deformation mechanisms themselves must be studied to better understand the impact of microstructure on mechanical properties. The goal of this work is to fill in these knowledge gaps using in-situ neutron diffraction and comparing grain orientation-dependent plastic deformation to quantify the effects of precipitate size and morphology on the various deformation mechanisms. This will allow for a better understanding of the effects of aging on mechanical properties at the grain scale.

### 29.2 Previous Work

#### 29.2.1 Microscopy Studies of Al-Cu Precipitate Evolution

The evolution of precipitates in Al-Cu follows a four-step process [29.3]. This process proceeds from supersaturated solid solution (SSS) → Guinier-Preston I zone (GPI zone) → GPII zones/θ″ → θ′ → θ. GPI and GPI/θ″ precipitates are disk-shaped, with habit planes on the (100) Al planes and fully coherent interfaces. θ′ is also disk-shaped on a (100) habit plane, having coherent faces and semicoherent edges. θ is spherical and fully incoherent with the matrix.

While this precipitation pathway is well defined, the mechanisms and kinetics are complex and not completely understood. There is some disagreement in the precipitation reactions, where θ′ precipitates may nucleate directly on θ″ precipitates, on vacancy clusters, or dislocation loops [29.4]. θ precipitates also seem to have multiple mechanisms of formation, nucleating either in the matrix directly, or on existing θ′ particles [29.5]. In situ transmission electron microscopy (TEM) has been done by C. Liu *et al.*; these results are helpful in the visualization of these processes [29.6].

Post-aging TEM has been applied in previous work at each of the aging conditions tested in the neutron diffraction beam. This will allow for observations of mechanical properties as a direct function of microstructure, as the mechanisms and kinetics of aging in Al-Cu alloys has already been studied in depth elsewhere [29.4,29.5,29.7–29.10]. Current work has not focused on mechanisms of precipitation and growth. However, future work may include 4-D characterization of nucleation and growth in these Al-Cu alloys with advanced x-ray characterization techniques.

#### 29.2.2 Qualification of Deformation Mechanisms *via* Time-of-Flight *In Situ* Neutron Diffraction

Time-of-flight (TOF) in situ neutron diffraction is a powerful tool for studying deformation in polycrystalline alloys. It can allow for the study of elastic (lattice) strains in individual grain orientations, which can be used to qualify deformation mechanisms as the material is strained [29.11]. The VULCAN beam line at the Spallation Neutron Source in Oak Ridge National Laboratory is used in this study, which includes a tensile frame and two detectors at 45 degree angles from the tensile direction.

Useful quantities that may be measured using this instrument include peak positions, the extent of peak broadening, and peak intensity changes. These quantities refer to the diffraction peaks in a neutron count (intensity) versus time of flight (position) plot, and can be used to measure lattice strain (essentially internal elastic strain), dislocation densities, and texture development. Results of these quantities will be explained later in this report.

### 29.3 Recent Progress

#### 29.3.1 Research Activities

A talk entitled “Identification of Deformation Mechanisms in Cast Al-Cu Alloys *via* Neutron Diffraction” was given by Brian Milligan at the 2018 TMS Annual Meeting. A peer-reviewed journal paper entitled “The Effect of Microstructural Stability on the Creep Behavior of Cast Al-Cu Alloys at 300 °C” is in preparation. A General User Proposal entitled “Three- and Four-Dimensional Characterization of Precipitate Evolution in Al-Cu and Al-Ag

Alloys" was submitted to Argonne National Laboratory's Advanced Photon Source to perform 3-D and 4-D transmission x-ray microscopy.

### 29.3.2 Transmission Electron Microscopy

As can be seen in **Fig. 19.1**, the aging conditions represent a range of Al-Cu precipitate evolution steps. The microstructures are summarized in **Table 19.1**. The precipitate evolution follows the expected order of SSS → GPI zone → GPII zone → θ″ → θ′ → θ. The as-quenched microstructure contained some GPI zones (most likely due to natural aging), the as-aged microstructure contained GPI and GPII zones, the 200 and 250°C preconditioned microstructures contained primarily θ′, and the 300°C preconditioned microstructure contained mostly θ with some θ′. The mixture of precipitates may complicate the deconvolution of deformation mechanisms. There will most likely not be a single mechanism responsible for the deformation in each condition. Therefore, either the evolution of the dominant mechanism (when possible), or mechanisms (e.g. from precipitate cutting to Orowan looping as particles grow) will be discussed later.

### 29.3.3 Neutron Diffraction

Tensile test results are presented in **Fig. 19.2**. As can be seen, the as-aged condition is the strongest, followed by the 200°C preconditioned, as-quenched, 250, and 300°C preconditioned. The only unexpected result here is the as-quenched sample. The previous thought was that the as-quenched sample would be primarily solid solution strengthened, but some of the TEM results suggest precipitation of GPI zones, which are most likely responsible for this strengthening effect.

Lattice stress versus macroscopic strain results are presented in **Fig. 19.3**. Lattice stress was calculated with literature values of Young's modulus and lattice strain measurements taken directly from diffraction data. The most interesting trend is the switch from isotropic strain hardening to anisotropic strain hardening, which then reverts back. The lack of strain hardening observed in the <200> oriented grains in the as-aged, 200, and 250°C preconditioned samples suggests that precipitate cutting is occurring in these grain orientations. The current hypothesis is that the as-quenched GP zones are so small that they have little effect on the strain hardening, and the majority of the precipitates in the 300°C preconditioned sample are so large that Orowan looping becomes the dominant deformation mechanism. The dominant deformation mechanisms are summarized in **Table 19.1**.

Another interesting result is the grain rotation. The diffracted intensity versus macroscopic strain is shown in **Fig. 19.4**. Note the decrease in intensity in the <220> oriented grains and the increase in intensity in the <111> oriented grains. This is expected behavior for an FCC single crystal [12], and is unsurprising that it occurs in this large-grained material.

## 29.4 Plans for Next Reporting Period

An outline of planned work for the next reporting period is shown below.

- Data analysis of high temperature neutron diffraction results on a more thermally stable alloy;
- Submit the journal paper entitled "The Effect of Microstructural Stability on the Creep Behavior of Cast Al-Cu Alloys at 300 °C";
- Perform aging studies at the Advanced Photon Source at Argonne National Laboratory, pending approval of a recently submitted user proposal;
- Prepare and submit a journal paper focused on the effect of microstructural changes on room-temperature mechanical properties in 206 Al alloy implementing neutron diffraction
- Perform additional creep testing in alternative Al-Cu alloys;
- Summer internship at ORNL.

## 29.5 References

[29.1] S. Roy, L.F. Allard, A. Rodriguez, T.R. Watkins, A. Shyam, Comparative Evaluation of Cast Aluminum Alloys for Automotive Cylinder Heads: Part I—Microstructure Evolution, Metall. Mater. Trans. A Phys. Metall. Mater. Sci. 48 (2017) 2529–2542. doi:10.1007/s11661-017-3985-1.

[29.2] S. Roy, L.F. Allard, A. Rodriguez, W.D. Porter, A. Shyam, Comparative Evaluation of Cast Aluminum Alloys for Automotive Cylinder Heads: Part II—Mechanical and Thermal Properties, Metall. Mater. Trans. A Phys. Metall. Mater. Sci. 48 (2017) 2543–2562. doi:10.1007/s11661-017-3986-0.

[29.3] J.L. Murray, The aluminium-copper system, Int. Met. Rev. 30 (1985) 211–234. doi:10.1179/imtr.1985.30.1.211.

[29.4] A. Suzuki, H. Kimura, Nucleation o f 0’ Precipitates in an Al-4% Cu Alloy, Mater. Sci. Eng. 6 (1970) 384–390.

[29.5] D. Vaughan, J.M. Silcock, The Orientation and Shape of ?? Precipitates Formed in an Al???Cu Alloy, Phys. Status Solidi. 20 (1967) 725–736. doi:10.1002/pssb.19670200235.

[29.6] C. Liu, S.K. Malladi, Q. Xu, J. Chen, F.D. Tichelaar, X. Zhuge, H.W. Zandbergen, In-situ STEM imaging of growth and phase change of individual CuAlX precipitates in Al alloy, Sci. Rep. 7 (2017) 2184. doi:10.1038/s41598-017-02081-9.

[29.7] V. Vaithyanathan, C. Wolverton, L.Q. Chen, Multiscale modeling of θ′ precipitation in Al-Cu binary alloys, Acta Mater. 52 (2004) 2973–2987. doi:10.1016/j.actamat.2004.03.001.

[29.8] A. Biswas, D.J. Siegel, C. Wolverton, D.N. Seidman, Precipitates in Al-Cu alloys revisited: Atom-probe tomographic experiments and first-principles calculations of compositional evolution and interfacial segregation, Acta Mater. 59 (2011) 6187–6204. doi:10.1016/j.actamat.2011.06.036.

[29.9] L. Löchte, A. Gitt, G. Gottstein, I. Hurtado, Simulation of the evolution of GP zones in Al-Cu alloys: an extended Cahn-Hilliard approach, Acta Mater. 48 (2000) 2969–2984. doi:10.1016/S1359-6454(00)00073-2.

[29.10] L.B. Ber, Accelerated artificial ageing regimes of commercial aluminium alloys. II: Al-Cu, Al-Zn-Mg-(Cu), Al-Mg-Si-(Cu) alloys, Mater. Sci. Eng. A. 280 (2000) 91–96. doi:10.1016/S0921-5093(99)00661-9.

[29.11] K. An, H.D. Skorpenske, A.D. Stoica, D. Ma, X.L. Wang, E. Cakmak, First in situ lattice strains measurements under load at VULCAN, Metall. Mater. Trans. A Phys. Metall. Mater. Sci. 42 (2011) 95–99. doi:10.1007/s11661-010-0495-9.

[29.12] J.H. Han, K.K. Jee, K.H. Oh, Orientation rotation behavior during in situ tensile deformation of polycrystalline 1050 aluminum alloy, Int. J. Mech. Sci. 45 (2003) 1613–1623. doi:10.1016/j.ijmecsci.2003.11.003.

**29.6 Figures and Tables**

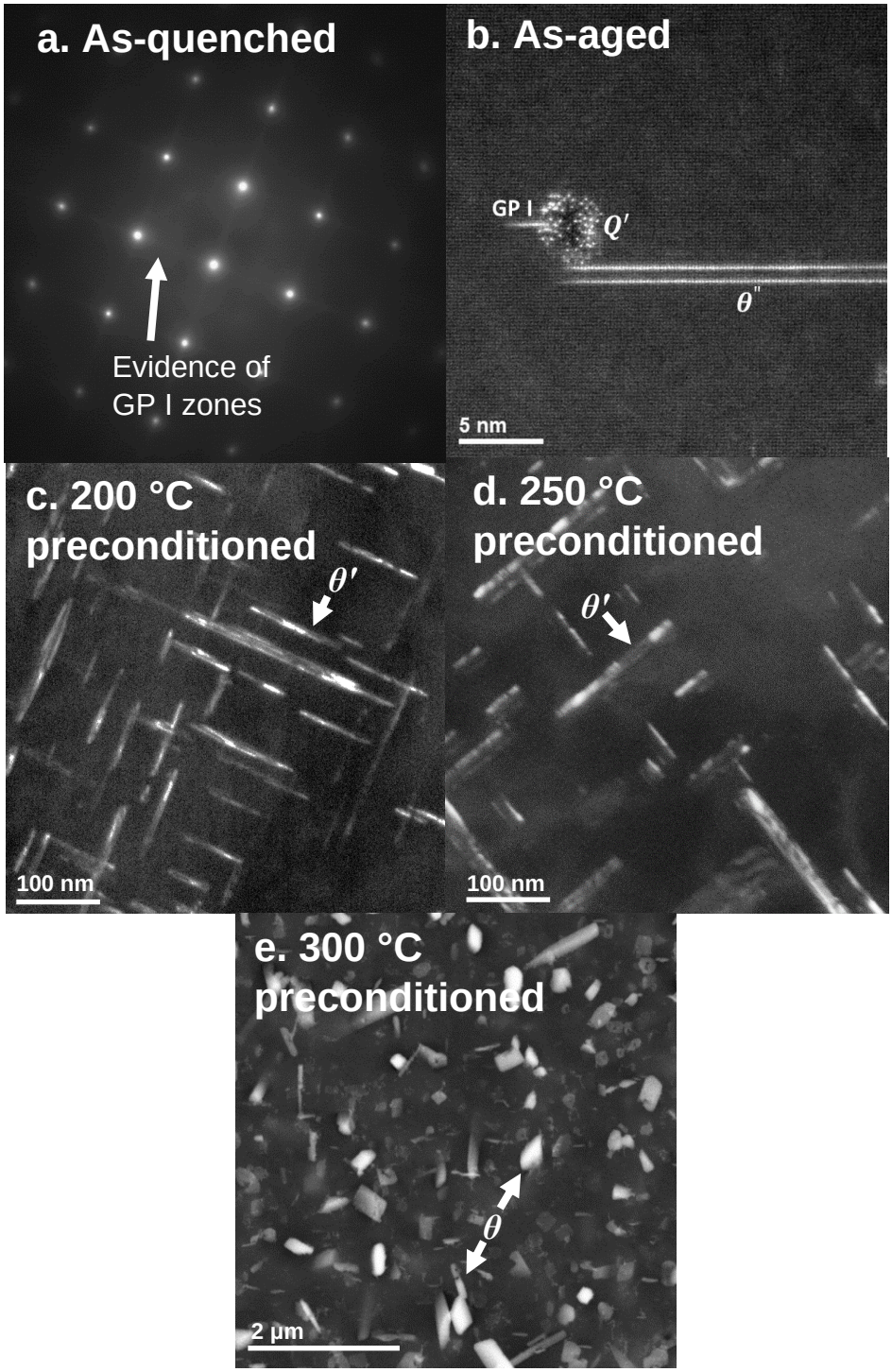


Figure 19.1: a. TEM diffraction pattern of the as-quenched condition. Zone axis in all images is (001). Streaking can be seen between the (001) type spots, indicating GPI zone formation. b. HR-STEM HAADF image of the as-aged condition, with nanoscale precipitates including GPI and GPII zones. c, d. TEM dark field images of 200 and 250 °C preconditioned samples, respectively. Primary precipitate in these conditions is θ′. e. FEG-SEM image of 300 °C preconditioned sample, with primarily θ precipitates.

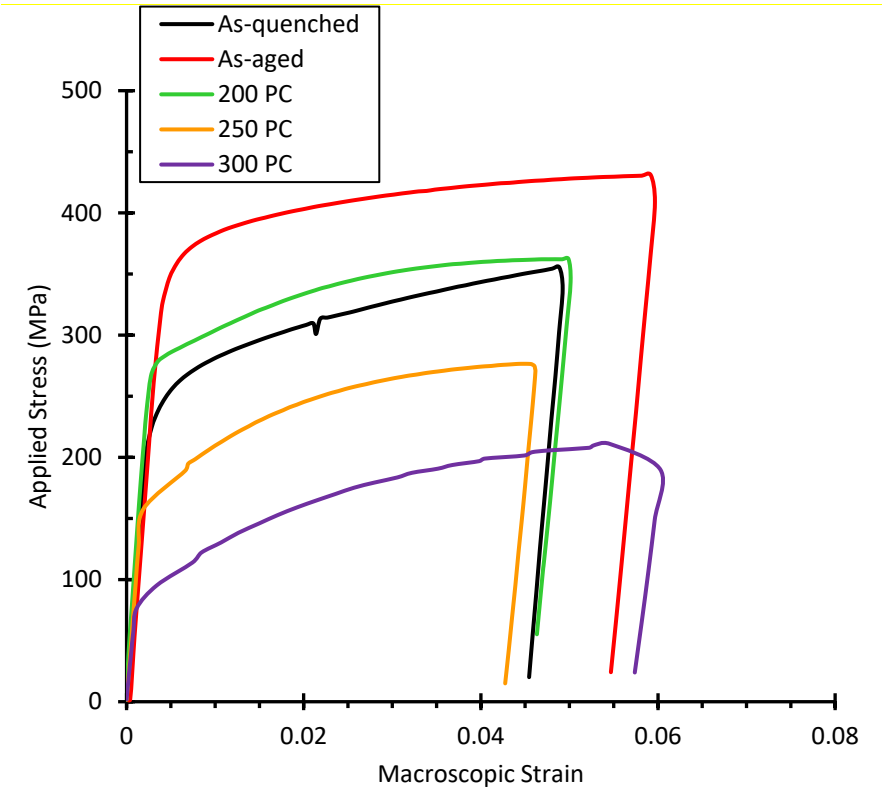


Figure 19.2: Applied engineering stress versus engineering strain (measured with an extensometer) plots for tensile tests of as-quenched, as-aged, and 200, 250, and 300°C preconditioned microstructures. Experiments were performed under the neutron beam. Imposed strain rate was $10^{-5}$ $s^{-1}$. Note no samples were taken to failure.

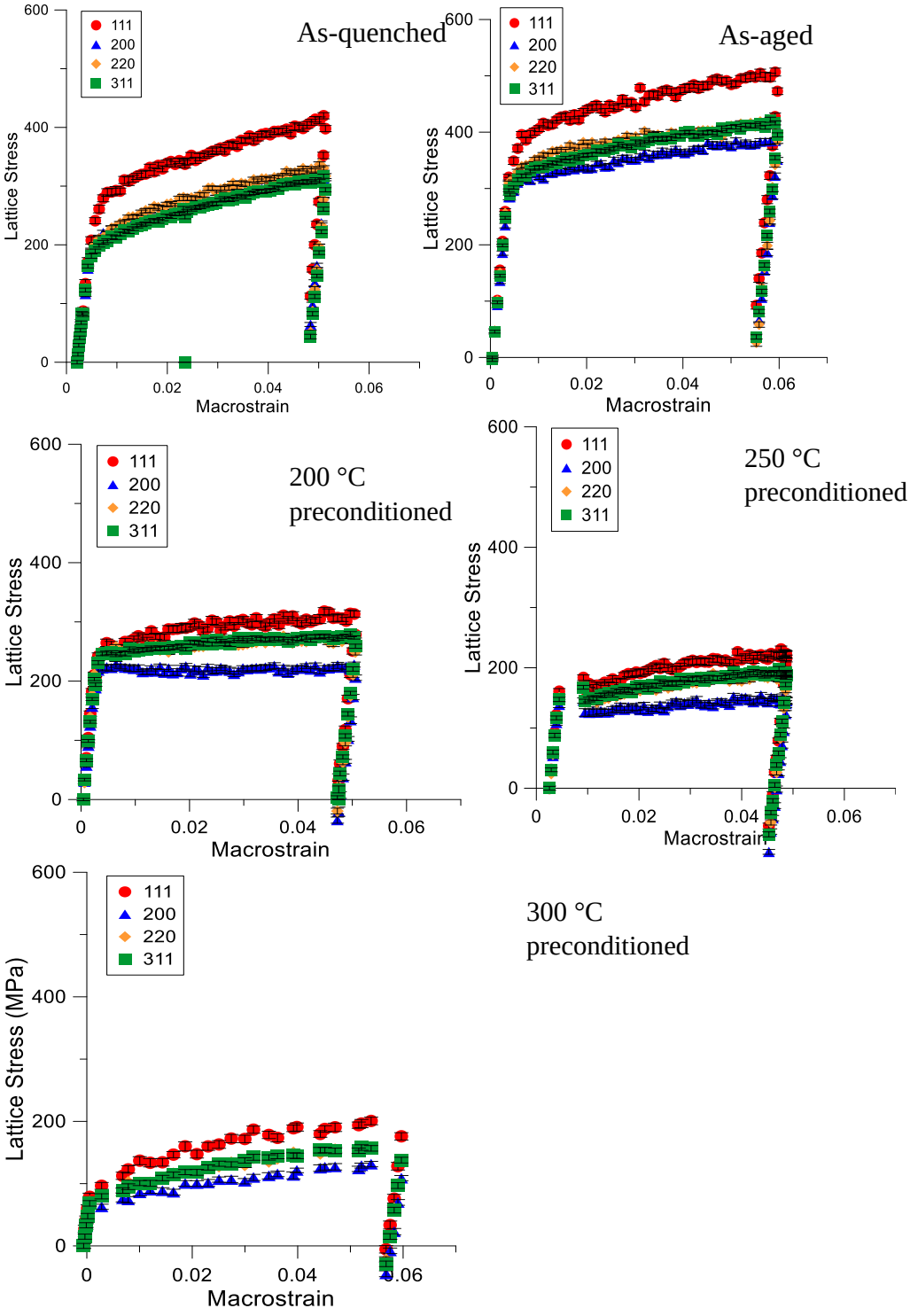


Figure 19.3: Summary of lattice stress vs. strain results from neutron diffraction. Note the isotropy in strain hardening in the as-aged and 300 °C preconditioned samples, and the anisotropy in strain hardening in the 200 and 250 °C preconditioned sample. This can be taken as evidence for preferential precipitate shearing in some grain orientations in these conditions.

Table 19.1: Precipitate morphologies at various aging conditions and primary strengthening mechanisms in these conditions.

| **Aging condition** | **Major precipitates** | **Approximate size** | **Possible strengthening mechanisms** |
|---|---|---|---|
| As-quenched | GPI | 10 Å thickness x 5 nm diameter | Solid solution strengthening, precipitate cutting |
| As-aged | GPI, GPII/θ″ | 2 nm thickness x 50 nm diameter | Precipitate cutting |
| 200°C Precondition | θ′ | 5 nm thickness x 200 nm diameter | Precipitate cutting |
| 250°C Precondition | θ′ | 10 nm thickness x 300 nm diameter | Precipitate cutting,<br>Orowan looping |
| 300°C Precondition | θ′, θ | 10 μm diameter | Orowan looping |